Advances in Synchrotron Radiation
Vol. 1, No. 2 (2008) 151–157

World Scientific
www.worldscientific.com

IN SITU TIME RESOLVED LAUE DIFFRACTION DURING MICRO-COMPRESSION EXPERIMENTS

ROBERT MAAß, STEVEN VAN PETEGEM,
HELENA VAN SWYGENHOVEN*, DANIEL GROLIMUND
and PETER M. DERLET

Paul Scherrer Institute, Villigen PSI
CH-5232, Switzerland
**helena.vanswygenhoven@psi.ch*

CYNTHIA VOLKERT

Forschungszentrum Karlsruhe, Karlsruhe D-76021, Germany

We present *in situ* and *ex situ* Laue micro-diffraction experiments on micron-sized single crystal pillars. We show that the focused ion beam technique introduces measurable damage in Si pillars. The dynamics of the Laue patterns of Au pillars demonstrate the occurrence of crystal rotation and strengthening is explained by plasticity starting on a slip system that is geometrically not predicted but selected because of the character of the pre-existing strain gradient.

Keywords: Laue micro-diffraction; *in situ* micro-compression; focused ion beam.

1. Introduction

Size effects in plasticity resulting from the reduction in specimen size have received much attention in recent years since conventional theories do not explicitly incorporate geometrical length-scale dependencies. In order to circumvent the coupled effects of strain gradients, as are encountered in nanoindentation and wafer curvature testing, micro-compression testing is often used as a technique to study the effects of geometric size.[1–4] In these experiments pillars with diameters on the order of tens of microns down to 100 nm are compressed using a nanoindenter outfitted with a flat punch indenter. The results show a general trend of increasing strength with decreasing diameters. Rationale for such behavior is greatly debated, with emerging theories including dislocation exhaustion and stochastic, scale-free dislocation mechanisms.[2,3,5,6]

Such pillars are typically fabricated using focused ion beam (FIB) machining from a thin film or bulk specimen. It is well-known that in metals FIB causes damage due to the Ga implantation.[7] However it is often assumed that such damage is restricted to a small surface region and that the FIB procedure does not alter the mechanical properties.

Computational simulations are currently being carried out in order to explore the origin of the observed geometric length scale size effect.[8] Up till now only macroscopic mechanical data and SEM observations are available as experimental input parameters for such simulations whereas very little is known about the evolving microstructure during compression. Furthermore it is assumed that the geometrical boundary conditions of the testing technique do not promote self organization and multiplication of dislocations leading to, for example, classical crystal rotation.[4,5,9]

To shed light on the initial microstructure and on possible FIB damage we have performed *ex situ* Laue micro-diffraction on Si pillars made both by FIB milling and by deep reactive ion etching.

We furthermore present an *in situ* time resolved Laue micro-diffraction experiment that captures the changes in microstructure during deformation of Au pillar.[10] The dynamics of the Laue patterns show that the initial strengthening seen in the smaller pillars can be explained by plasticity starting on a slip system that is geometrically not predicted but selected because of the character of pre-existing strain gradients within the sample. Moreover as the plasticity proceeds, significant rotation of the crystal is observed.

2. Experimental

2.1. *Sample preparation*

Si pillars were made by FIB milling and by deep reactive ion etching (DRIE, SF_6 plasma for etching, C_4F_8 for passivation). Details about the synthesis method can be found in Ref. 11. Pt markers under the pillars facilitate alignment using fluorescent mapping.

Au pillars were prepared by FIB milling. A large grained Au foil placed on a sample holder with its surface-normal oriented horizontally was first locally thinned to a final thickness of $\sim 20\,\mu$m. Grains were detected by electron backscattered diffraction and by a multi-step procedure, larger cylindrical base structures were cut. The final step included the FIB-machining of the pillar, which was cut out from the top part of the base structure, resulting in a row of free standing samples all having the same top.

2.2. *Laue geometry*

Polychromatic diffraction patterns were measured in Laue transmission geometry with photon energies ranging from 2 to 24 keV. Kirkpatrick–Baez mirror focusing optics was used to obtain a beam FWHM of 1.5–2.5 μm^2 in the focal plane with a maximum angular divergence of 0.2×0.3 mrad. A large area charged-coupled-device (CCD) detector (Photonic Science, FDI-VHR 150) with 3862×2526 pixel resolution was placed perpendicular to the beam direction. All the Si and Au pillars are positioned such that the diffracted beam has a spatial freedom of more than 40°.

2.3. *In situ setup*

The *in situ* compression experiments were conducted with a micro-compression device (MCD), designed to be mounted on the rotational stage of the six-axis sample manipulator at the micro-XAS beamline at the Swiss Light Source. The MCD consists of several independent piezo stages allowing correct positioning of the compression head. For the compression head, a truncated conical diamond indentation tip with 60° opening angle and end tip radius of 11 μm was used. Several setscrews served for control of tilt between the sample and the compression head. All manipulations of the compression head and the sample as well as the touch down procedure and compression are monitored with high resolution optical microscopes.

The MCD is equipped with a Hysitron TriboScope© single axis transducer, which generates both load and displacement via the applied voltage on the three-plate capacitive transducer. During the *in situ* measurements Laue patterns were continuously measured, with exposure times of the order of 10–20 s, and later correlated with the mechanical data obtained from the TriboScope transducer.

3. Results and Discussion

3.1. *Influence of FIB*

In order to investigate the influence of the pillar fabrication method several diffraction patterns were taken of the pillars and compared to patterns taken at the area below the pillar. Figure 1 shows the contour plots of the (1−33) diffraction spot, the behavior of the other diffraction spots being similar. Figures 1(a) and 1(c) were acquired for, respectively, Si-DRIE and Si-FIB at an area well below the pillar. In both cases the shapes of the diffraction spots are isotropic and are comparable with diffraction spots taken from a reference Si wafer.

The shapes of the (1−33) diffraction spots taken at the center of the pillars are shown in Figs. 1(b) and 1(d) for, respectively, Si-DRIE and Si-FIB. In the case of Si-DRIE no differences with the diffraction spots of the bulk could be found. This is an indication that the DRIE process did not introduce significant damage. In contrast the (1−33) diffraction spot of Si-FIB exhibits clear streaking. However the intensity of the streaks is relatively low compared to the intensity of the main

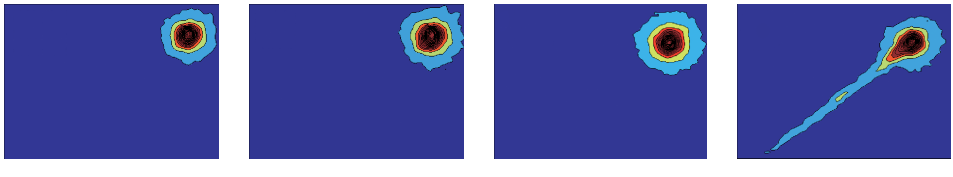

(a) (b) (c) (d)

Fig. 1. Contour plots of the (1−33) diffraction spot for the bulk region of Si-DRIE (a) and of Si-FIB (c), and for the pillars of Si-DRIE (b) and of Si-FIB (d) (color online).

diffraction peak, suggesting that the volume of the damaged region causing the streaking is relatively small.

It is well-known that FIB milling of Si creates a surface amorphous layer,[12] as well as Ga incorporation, which could lead to a complex strain distribution within the pillar. The observed amount of streaking could be explained by anisotropic elastic strain distributions within the pillar, but to rule out contributions of excess dislocations or pure rotational effects due to for instance recrystallization of an amorphous layer,[12] further investigations are needed.

3.2. *In situ mechanical testing*

Figure 2 shows the stress–strain curves of a 2 μm Au pillar that has been deformed while continuously recording Laue patterns. The deformation curve is characterized by an initial elastic part followed by rapid strain bursts. Post-mortem surface investigation shows slip traces according to the (1−11), the (1−1−1) and the (−1−11) slip planes. The strength of the pillar is clearly larger than what is expected for a bulk Au single crystal and in agreement with values found in literature for a 2 μm Au pillar.[3]

The white beam Laue transmission diffraction pattern recorded prior to deformation contains five diffraction spots of sufficient intensity corresponding to the reflections (−200), (02−2), (−31−1), (−1−31) and (−22−2). They all exhibit continuous streaking indicating the presence of a strain gradient. This is evidenced for the (02−2) diffraction spot in Fig. 3(a). Upon compression all Laue spots evidence additional continuous streaking until just before the first strain burst is observed (Fig. 3(b)). Following Barabash *et al.*,[13] the observed streaking can be assigned to the presence of unpaired dislocations with a Burgers vector [0−1−1] lying in the

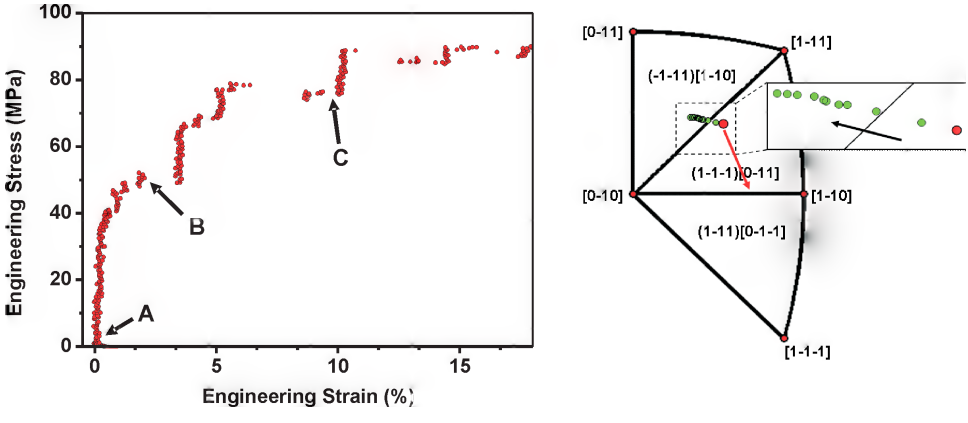

Fig. 2. (left) Engineering stress–strain curve of a 2 μm Au pillar. (right) Inverse pole figure showing crystal rotation via the evolution of the compression axis in the reciprocal space of the pillar. The orientation before deformation (∼[4−63]) is indicated by the larger red circle. Figure taken from Ref. 10 (color online).

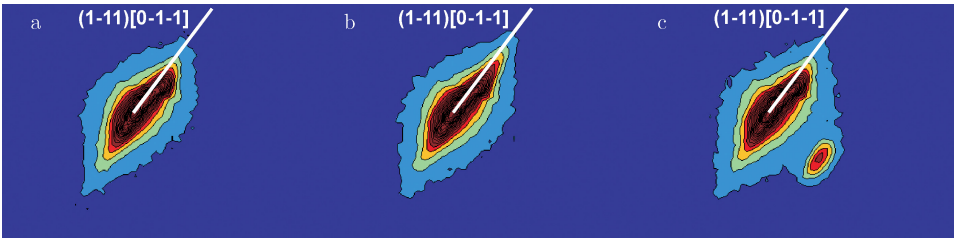

Fig. 3. Contours plots of the (−22−2) diffraction spot before deformation (a), at 40 MPa (b) and at 77 MPa (c) as indicated on the stress/strain curve in Fig. 1. The white line indicates the expected streaking direction for the case of an excess of unpaired edge dislocations on the (1−11)[0−1−1] slip system (color online).

(1−11) slip plane as indicated by the white lines in Fig. 3. It should be noted that this is a slip system with a low Schmid factor. At the moment of the first strain burst streaking of the Laue spot reduces. In other words, upon loading an ensemble of dislocations is formed that will self-organize to a critical slip process visible by a strain burst, bridging the gap between individual dislocations and an ensemble of dislocations preparing for macroscopic plasticity.[6]

When the applied load reaches a value of 77 MPa another large strain burst is observed coinciding with the take off of satellite peaks (Fig. 3(c)). Between the first strain burst and the formation of the satellite peak, the Laue streaking reduces further and the final width of the mother peak is narrower compared to the width prior to loading, demonstrating a partial strain gradient relief in the pillar.

The paths of all satellite diffraction peaks during deformation uniquely define a rotation of the crystal. The direction the satellite takes off is situated in between the directions to be expected for slip along (1−1−1)[0−11] and slip along (−1−11)[1−10], suggesting that at this strain these two slip systems are already operating. Figure 2 shows, using an inverse pole plot of the primary triangle formed by the [0−10], [1−10] and the [1−11] poles, the evolution of the crystal rotation by plotting the vertical axis in the reciprocal space of the crystal.[24] The geometrically predicted slip systems are shown for the primary and neighboring triangles. For compression geometries where the crystal is free to rotate, the vertical axis should rotate towards the line [0−10]−[1−10] using the (1−1−1)[01−1] slip system (indicated by the red arrow in the inverse pole figure shown in Fig. 2), where upon the (1−11)[0−1−1] system is equally activated maintaining the orientation along the [0−10]−[1−10] line. However for the smallest pillar, the crystal rotates in the opposite direction, continuing towards the line [0−10]−[0−11] after having crossed the [0−10]−[1−11] line.

Our time resolved observations demonstrate that a two-micron pillar initially oriented for slip along one geometrically favoured system deforms by selecting a different slip system that is 1.5 times harder, a choice that can be explained by the importance and the directionality of the initial strain gradient. With bigger

pillars less influenced by the initial strain gradient a "smaller is stronger" trend is therefore not such a surprise. The *in situ* experiment furthermore shows that upon loading, the diffraction peaks streak additionally along the pre-existing streaking direction, suggesting a dislocation breeding as a preface to the first strain burst. Slip along the hard system in the two-micron pillar relieves internal strain after which other slip systems are activated. It is worth to note that such a scenario could be also interpreted in terms of a classical dislocation pile-up against a surface layer as was suggested for the strengthening in five-micron Al wires,[14] with in addition here, that the selection of the slip system is determined by the pre-existing strain gradient induced during FIB sample preparation, a method that might also introduce a surface layer. Staying in the classical picture, the higher flow stress needed for the following strain bursts can be ascribed to latent hardening[15] as a result of alteration of different slip systems.

4. Conclusions

Ex situ Laue micro-diffraction on Si pillars fabricated by dry etching and by FIB demonstrates that the latter technique induces measurable strain gradients. The influence of strain gradients on the mechanical properties of small Au pillars synthesized using FIB is demonstrated by *in situ* time resolved Laue diffraction. It is shown that (1) plasticity starts on a slip system that is geometrically not predicted, but selected because of the character of the pre-existing strain gradients, (2) the deformation method involves crystal rotation, and (3) the presence of a dislocation breeding mechanism prior to a strain burst. The results obtained underline the necessity of an *in situ* method that follows the underlying microstructure during deformation, in order to understand the "smaller is stronger" trend and provide invaluable input for mesoscopic modelling.

Acknowledgments

HVS thank the Swiss National Science Foundation (SNF-2100-065152.01) and the European Commission (FP7-NANOMESO) for financial support. The authors also thank Dr. E. Lilleodden, M. Willimann, A. Bollhalder and M. Schild for their support, S. Brandstetter and Dr. B. Schmitt for helping during beamtime measurements. Further gratitude is expressed to Dr. U. Hangen and M. Berg from Hysitron Incorporated for supporting the TriboScope© implementation.

References

1. M. D. Uchic, D. M. Dimiduk, J. N. Florando and W. D. Nix, *Science* **305**, 986 (2004).
2. J. R. Greer, W. C. Oliver and W. D. Nix, *Acta Mater.* **53**, 1821 (2005).
3. C. A. Volkert and E. T. Lilleodden, *Phil. Magazine* **86**, 5567 (2006).
4. M. D. Uchic and D. A. Dimiduk, *Mater. Sci. Eng. A – Struct. Mater. Properties Microstruct. Process.* **400**, 268 (2005).
5. D. M. Dimiduk, M. D. Uchic and T. A. Parthasarathy, *Acta Mater.* **53**, 4065 (2005).

6. D. M. Dimiduk, C. Woodward, R. LeSar and M. D. Uchic, *Science* **312**, 1188 (2006).
7. C. R. Hutchinson, R. E. Hackenberg and G. J. Shiflet, *Ultramicroscopy* **94**, 37 (2003).
8. V. S. Deshpandea, A. Needleman and E. Van der Giessen, *Mater. Sci. Eng. A – Struct. Mater. Properties Microstruct. Process.* **400**, 393 (2005).
9. H. Zhang, B. E. Schuster, Q. Wei and K. T. Ramesh, *Scripta Mater.* **54**, 181 (2006).
10. R. Maaß, S. Van Petegem, H. Van Swygenhoven, P. M. Derlet, C. A. Volkert and D. Grolimund, *Phys. Rev. Lett.* **99**, 145505 (2007).
11. R. Maaß *et al.*, *Appl. Phys. Lett.* **89**, 151905 (2006).
12. S. Rubanov and P. R. Munroe, *J. Microscopy – Oxford* **214**, 213 (2004).
13. R. I. Barabash, G. E. Ice and F. J. Walker, *J. Appl. Phys.* **93**, 1457 (2003).
14. T. Tabata, H. Fujita, S. Yamamoto and T. Cyon, *J. Phys. Soc. Jpn.* **40**, 792 (1976).
15. S. J. Basinki and Z. S. Basinki, *Dislocations in Solids*, Vol. 4, ed. F. R. N. Nabarro (North-Holland, Amsterdam, 1979), p. 261.